JOURNAL OF MATERIALS SCIENCE 19 (1984) 1760–1766

Crystallization and properties of glasses prepared from Illinois coal fly ash

EILEEN J. DeGUIRE*, SUBHASH H. RISBUD
Department of Ceramic Engineering and Materials Research Laboratory, University of Illinois at Urbana-Champaign, 105 S. Goodwin Avenue, Urbana, Illinois 61801, USA

Glasses synthesized from Illinois coal fly ash by conventional melt quenching were recrystallized by suitable nucleation and crystal growth heat treatments. The microstructure and selected properties of the glasses and crystallized glasses were investigated using scanning and scanning transmission electron microscopy (SEM, STEM), Mössbauer spectroscopy, differential thermal analysis (DTA) and X-ray diffraction (XRD). Crystallization of the fly ash glasses without the aid of added nucleating agents was possible up to a maximum of ~ 23 vol %. The crystalline phase was tentatively identified on the basis of STEM microanalysis as a combination of ferroaugite [$(Ca, Fe^{2+})(Al, Fe^{3+})_2SiO_6$] and potassium melilite [$KCaAlSi_2O_7$]. Comparative results of the thermal expansion, density and microhardness of the glass and crystallized glass are reported along with the Young's modulus of a glass fibre pulled from the fly ash melt.

1. Introduction

Coal-burning plants exhaust large quantities of combusted waste in the form of bottom ash, fly ash, or slag which creates a disposal problem; for example, Illinois coals typically contain 12 to 15 wt % ash. Two types of ash result from the coal combustion process: bottom ash and fly ash. Bottom ash is fairly coarse with substantial amounts of uncombusted coal. Fly ash, on the other hand, is quite fine (micron size) and almost completely combusted although it, too, contains some residual carbon and sulphur. Both types of ashes are quite glassy due to the rapid quenching conditions that exist in the boiler furnace.

Fly ash has been used as aggregate for concrete, for soil stabilization and modification, as cinder on winter roads, as landfill, for brick manufacture, or as a raw material for mineral wool production. Attempts have been made to make abrasion-resistant ceramics by dry pressing and sintering the ash but this approach was found to be problematic because the residual carbon and sulphur tended to cause bloating during firing. Several studies of waste-ash utilization in glass and ceramic technologies have been reported in the literature [1–5]. The present research is a study of the preparation, crystallization and properties of glasses obtained by melting and quenching an Illinois coal fly ash composition.

2. Experimental procedure

Fused silica crucibles were charged with approximately 50 g fly ash obtained from the Illinois Power Company. The ash was melted at 1500° C for 2 h in a gas-fired furnace and then poured into shallow, 15 cm long graphite moulds. X-ray diffraction and DTA† were used to study glass characteristics; 2.5 cm sections were cut for recrystallization studies of the glass.

The microstructure and microchemistry of crystallized glasses were determined by scanning electron microscopy (SEM), and scanning transmission electron microscopy (STEM). Volume fractions crystallized upon heat treatment were estimated from enlargements of the micrographs obtained using the techniques described by Carrier [6] and Underwood [7]. Thermal expansion coefficients,†

* Present address: the Army Materials and Mechanics Research Center, Watertown, Massachusetts 02172, USA.
† DuPont 1090 Thermal Analyser.

0022–2461/84 $03.00 + .12

TABLE I Illinois coal fly ash composition

Oxide	(wt %)
SiO_2	47.6
Al_2O_3	29.6
Fe_2O_3	15.8
CaO	4.2
MgO	0.6
K_2O	1.7
Na_2O	0.5

densities [8] and Knoop microhardness* of glasses and recrystallized glasses were determined. Young's modulus was measured sonically on a glass fibre [9]. This technique could not, however, be used on the recrystallized glasses.

3. Results and discussion

3.1. DTA and crystallized microstructures

Table I lists the chemical analysis of the fly ash used in this study†, and Fig. 1 shows an example of a bulk fly ash glass in the as-prepared state. A DTA curve of the glass is shown in Fig. 2. The glass transition occurs at ~560° C in the DTA as also verified by thermal expansion measurements. Based on the DTA data, nucleation temperatures of 650 and 700° C were chosen for 2 h treatments followed by crystallization treatments at 800, 850, 900 and 950° C for 5 and 10 h. X-ray diffraction revealed that crystallites had started to form upon heat treatment but they were too small to be seen in the SEM implying nucleation had occurred without significant crystal growth. Since the DTA trace seems to indicate that crystallization occurs in the presence of a liquid phase, a second set of crystallization treatments were given to the glass at temperatures of 1000 and 1150° C for 2 and 4 h. The greatest extent of crystallization was found in samples heat treated at 1150° C for 4 h.

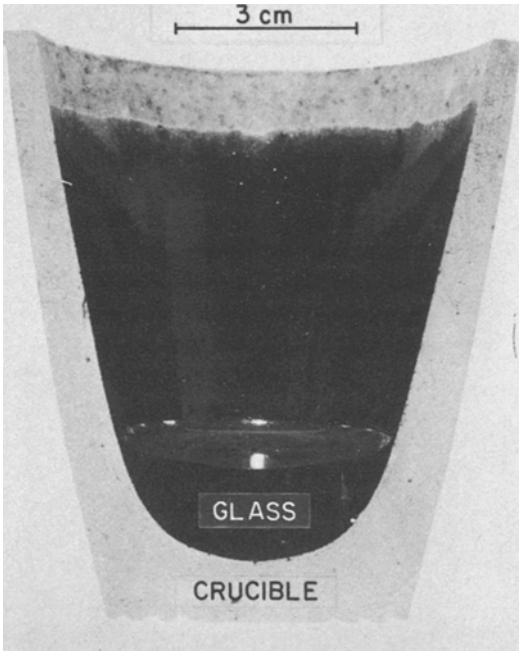

Figure 1 Photograph of bulk glass obtained by melting and cooling the fly ash composition in a silica crucible.

It was anticipated that the density of crystal nuclei would not be the same for all the samples since the nucleation rate is temperature dependent. Thus samples treated at 650 and 800° C were expected to have different density of nuclei than samples treated at 650 and 950° C. Similarly, nucleation treatments of 650 and 800° C were expected to result in a different number of nuclei than the 700 and 800° C treatments. Differences in the nuclei density can be expected when comparing the microstructures of samples subjected to identical subsequent crystal growth treatments.

X-ray diffraction data showed that the crystalline phase after the crystal growth treatment was identical to that obtained following the two-step nucleation treatments. Fig. 3 shows SEM micrographs of three samples subjected to different two-step nucleation treatments and identical crystal growth treatments. There is no detectable change in the volume fraction of the crystalline phase after the various nucleation treatments. Similar observations on other samples with different nucleation treatments also indicated that the volume fraction crystallized was not significantly affected by the nucleation treatments. A glass sample subjected to the crystallization heat treatment without a prior nucleation heat treatment had the same microstructure as the nucleated and crystallized samples suggesting that only the crystal growth treatment influences the crystallized microstructure. Quantitative analyses of the micrographs yielded an average crystallite size of 1.2 μm and a volume fraction crystallized of 23%.

3.2. Microanalysis of crystallized phases

Microchemical characterization by STEM was attempted to better identify the crystalline phase

* Tukon Microhardness Tester.

† Analysed by Coors Spectrochemical Laboratory, Golden, Colorado, USA.

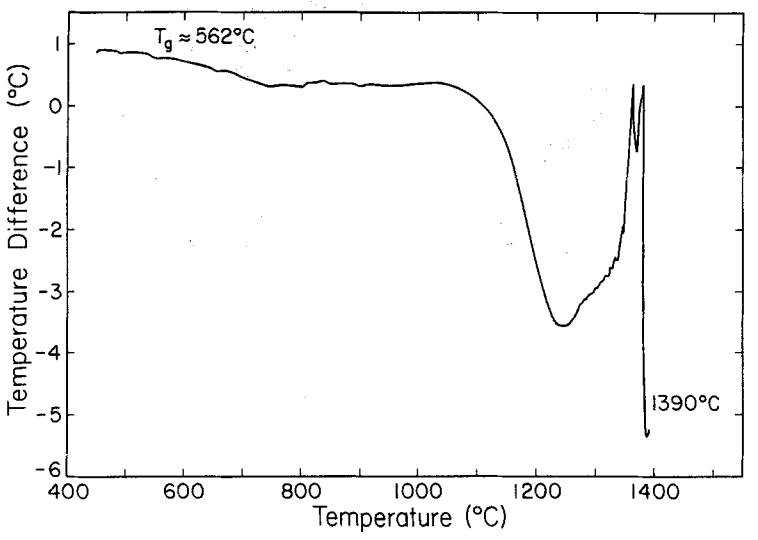

Figure 2 Differential thermal analysis (DTA) trace during heating of the as-prepared fly ash glass. (Heating rate = 10° C min^{-1}.)

precipitated in the glass-ceramics. The STEM analysis suggested that the crystallized glass probably contains two crystalline phases, pyroxene and potassium melilite. A pyroxene phase can be expected to form upon crystallization of these types of glass compositions. Rogers and Williamson [10] observed melilite in glass samples similar in composition to the present study and thus, the presence of potassium melilite is not without precedent. However, a certain identification of the crystalline phases was complicated by difficulties in obtaining uncontaminated ion-thinned foils for the STEM microanalysis and ambiguous X-ray diffractometer data. The STEM X-ray data collected from four separate locations on the ion-thinned specimen of the crystallized glass are summarized in Table II. The computerized X-ray analysis system could not differentiate between silicon and aluminium peak intensities, so they have been integrated into one. The results reported are cation per

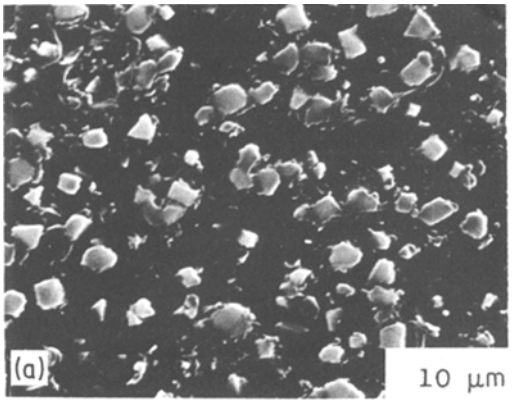

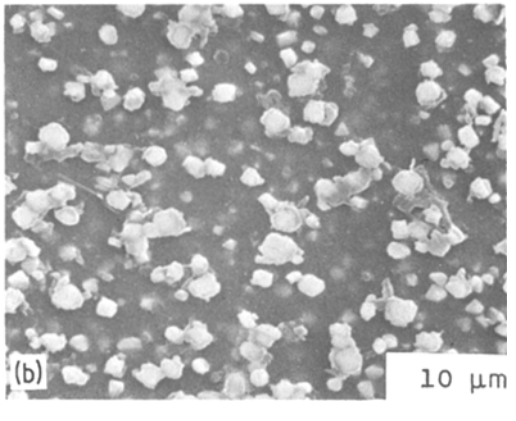

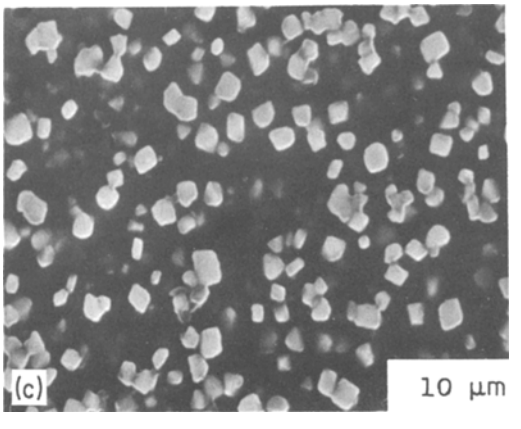

Figure 3 SEM photomicrographs of crystalline phases developed upon reheating fly ash glass samples under different nucleation and crystal growth conditions; (a) 1150° C, 4 h; (b) 650° C, 2 h + 950° C, 10 h + 1150° C, 4 h; and (c) 700° C, 2 h + 950° C, 10 h + 1150° C, 4 h.

TABLE II STEM X-ray analyses of crystallized glass

Element	(wt %)			
	1	2	3	4
Si + Al	86.12	79.60	78.96	41.74
K	0.73	2.06	2.58	6.50
Ca	2.24	3.47	4.07	8.31
Fe^{2+}	8.18	10.47	10.79	31.21
Fe^{3+}	2.73	3.49	3.59	10.40
Ti	–	0.92	–	1.84

cents and are accurate to approximately ± 5%. Table III shows the composition of the ash in cation per cents, (a) based on all cations known to be in the ash, and (b) based only on the silicon, aluminium, potassium, calcium and iron cations. The iron has been divided into Fe^{2+} and Fe^{3+} on the basis of Mössbauer spectroscopy results. The glass-ceramic STEM specimen was 75% Fe^{2+} and 25% Fe^{3+}.

Analyses 1 to 3 in Table II are most likely representative of the glass phase in view of the relatively higher silicon + aluminium content. This conclusion is also based on the similarity of the first three analyses to the ash composition. Analysis 4 in Table II is probably representative of the crystalline phase. Other researchers [10–13] studying compositions similar to that of the ash used in this research found that the major crystalline phase was a pyroxene. However, pyroxenes cannot incorporate potassium into their structures and analysis 4 shows a substantial amount of it in the crystalline phase. Rogers and Williamson [7] found gehlenite (which is melilite) in addition to the diopside in their crystalline samples and the melilites can readily accept potassium. Based on these data and a survey of the literature on potassium-containing phase diagrams [14], melilite with the chemical formula $KCaAlSi_2O_7$ was considered the most likely phase identified by the present analysis in addition to pyroxene.

TABLE III Ash composition

Element	(wt %)	
	A*	B†
Si + Al	80.09	81.61
K	2.14	2.18
Ca	4.37	4.45
Fe^{2+}	11.53	11.75
Na	2.02	–
Mg	0.83	–

*Based on all cations known to be present in ash (see Table I).
†Assuming ash contains Si, Al, K, Ca and Fe only.

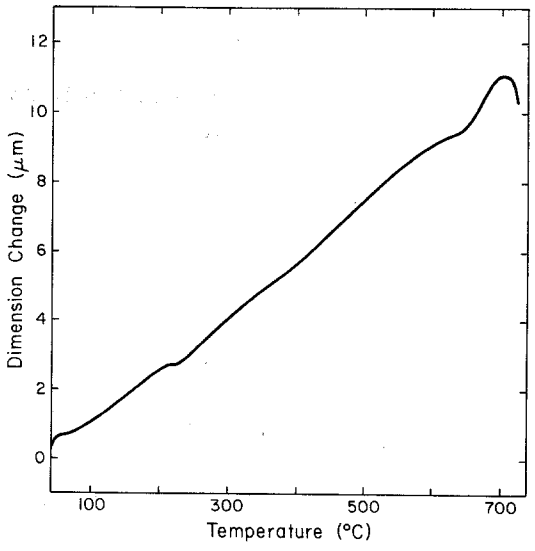

Figure 4 Typical thermal expansion curve for the fly ash glass.

After accounting for the potassium phase, the remaining cations were present in the appropriate amounts for a pyroxene phase with the chemical formula of $(Ca, Fe^{2+})(Al, Fe^{3+})_2SiO_6$. This phase has a very high iron content and falls in the ferroaugite phase field. That titanium was found in the crystalline phase is interesting and suggests that there is some TiO_2 in the ash which may act as a nucleating agent. The amount of TiO_2 in the glass must be very small (probably no more than 1 or 2 wt % in the light of the chemical analysis of the ash reported earlier, see Table I). The limited amount of crystallization observed in this study could well be due to the limited amount of TiO_2, thus suggesting that a nucleating agent might be essential to cause extensive crystallization of these fly ash glasses to glass-ceramic bodies.

3.3. Properties

3.3.1. Thermal expansion

A typical plot of the thermal expansion of the glass is shown in Fig. 4; the glass transition was estimated at ~565° C consistent with the glass transition temperature determined by DTA. The mean thermal expansion coefficients of the glasses and glass-ceramics at temperatures from 100 to 600° C range from 4.96×10^{-6} to 5.63×10^{-6} °C^{-1} with the glass being the lowest and the recrystallized glass being the highest. Therefore, it would

TABLE IV Properties of as-prepared and crystallized fly ash glasses

	Average thermal expansion ($\times 10^{6\circ} C^{-1}$)	Average Knoop hardness ($kg\,mm^{-2}$)	Average density ($g\,cm^{-3}$)	Young's modulus (GPa)
Glass	4.97 ± 0.51	555.5 ± 51.0	2.7133	86.86 ± 5.73
Nucleated glass	5.39 ± 0.81	445.9 ± 54.9	2.7552	–
Recrystallized glass	5.63 ± 0.70	458.6 ± 45.8	2.7309	–

seem that thermal expansion increases with an increasing amount of crystallinity. However, the scatter in the data was large and the standard deviations indicate that the increasing trend in the means may not be statistically significant. No significant change in thermal expansion upon crystallization can thus be concluded from the data. The scatter in the glass data could be due to structure differences between the glasses as a result of variations in the Fe^{2+}/Fe^{3+} ratio or due to composition differences between samples because of inhomogeneities in the bulk glasses.

3.2.2. Microhardness

As summarized in Table IV, the as-prepared ash glass had the highest microhardness while the nucleated glass had the least microhardness. The microhardness trend is consistent with what can be expected based on compaction, deformation and density considerations. The nucleated glasses were known to have microcrystallites in them, but they were so small that they could not be seen in the SEM. On the other hand, the Knoop indentation was easily seen in an optical microscope and was many orders of magnitude larger than the microcrystallites. Therefore, the microhardness of the nucleated glasses can be attributed to the properties of the glass phase and explained in terms of its density.

Knoop microhardness of the recrystallized glasses was less than that of the untreated glass and slightly greater than that of the nucleated glass. Since the indentation length is much larger than the average crystal size (about 1.2 μm), the hardness can probably be attributed to the overall density of the sample. Beall and Rittler [11] found that basalt glass-ceramics were harder than the glass from which they were formed but no density measurements were reported. The Knoop microhardness values reported by Beall and Rittler (650, 900 $kg\,mm^{-2}$) are greater than those found in this study, but since the load used was not specified, it is difficult to compare the magnitudes of the microhardness values in the two studies. Possible sources of error in microhardness measurements include variations in surface treatment, limitations in the microscope resolution and operator errors. All of the samples were polished the same way to minimize surface differences and all of the microhardness testing was done on the same day in order to minimize the possible errors.

3.3.3. Density and elastic modulus

The results of the density measurements on the heat treated glasses are shown in Fig. 5. The temperature plotted on the abscissa is the temperatures of the second nucleation heat treatment. The mean glass density was 2.7133 $g\,cm^{-3}$. The densities of the nucleated glasses vary, as expected, with nucleation temperature, i.e. density decreases as treatment temperature increases. These temperatures are well above the glass transition of 560° C. These trends are perhaps the result of the competing effects of densification due to structural rearrangement and thermal expansion. The contribution of thermal expansion is greater at the higher temperatures and thus the density is lower.

The effect of the time and temperature of the first nucleation treatment can also be seen in Fig. 5. Not surprisingly, the density of the samples treated for 10 h is greater than that of the samples treated for 5 h. This simply indicates that more than 5 h was needed for the maximum densification to occur. The comparison of the temperature effect is somewhat difficult to make since the viscosity of the glass at 700° C would be less than at 650° C so that structural relaxation would occur more readily at 700° C. At the same time, however, the net expansion of the glass at 700° C would be greater. The data do not indicate dominance of one effect over the other and the temperature of the first nucleation treatment seems to have no effect on density after all heat treatments. The density of the crystallized samples is less than the nucleated glasses but greater than the glass. The glassy phase, occupying the larger volume, will contribute more to the density than the crystal phase, but its density is unknown since

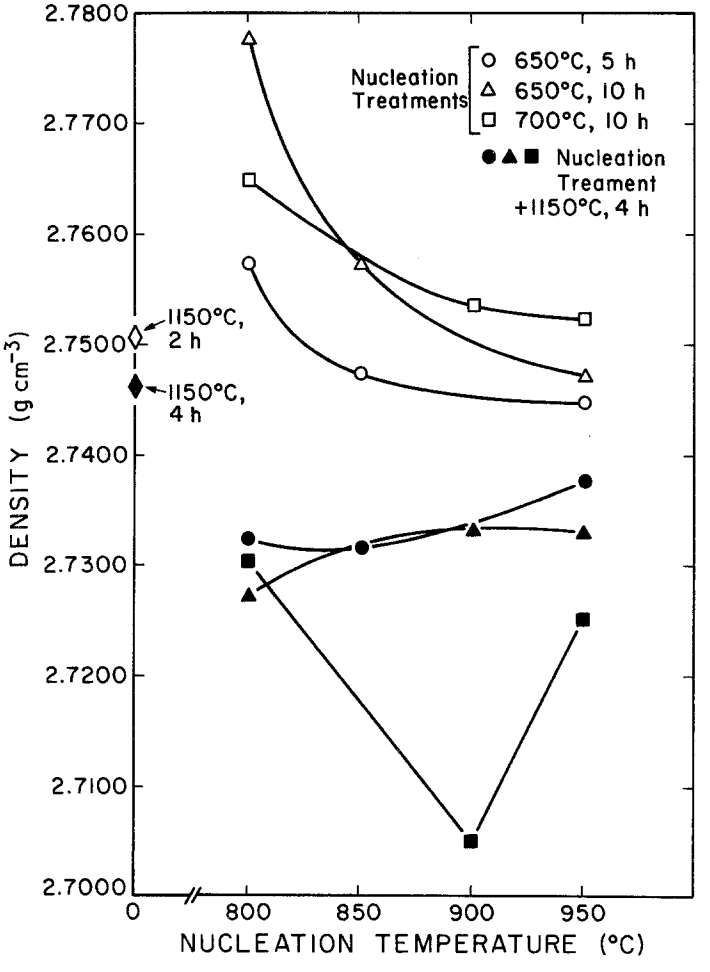

Figure 5 Measured densities of fly ash glass samples, after various crystallization schedules, plotted as a function of the second stage nucleation treatment temperatures.

the composition (and therefore the density) of the glass changes as the crystalline phase precipitates. There is a slight increasing trend in the densities of the crystallized samples with nucleation treatment and it is probably due to thermal expansion. That the trend is not very strong further supports the conclusion that the nucleation steps have little effect on the outcome of the crystallization heat treatment.

The Young's modulus of the ash glass was determined for a glass fibre by acoustic methods [9]. It was not possible to use the technique on heat-treated glasses. The measured Young's modulus was 86.86 ± 5.73 GPa; that of fused silica [15] is approximately 70 Gpa and that of steel [16] is approximately 200 GPa. It is estimated that the Young's modulus of a fibre is on the order of 5% less than Young's modulus of a bulk glass of the same composition. The property data obtained in this work are summarized in Table IV.

4. Conclusions

Glasses were readily synthesized from Illinois coal fly ash. They could be recrystallized through appropriate nucleation and crystal growth heat treatments, but they could not be recrystallized to more than approximately 23 vol%. STEM microanalysis suggests that this may be due to a limited amount of TiO_2 in the glass. The crystalline phases were tentatively identified as ferroaugite and potassium melilite. Several thermal and mechanical properties that are important in engineering design were measured.

Acknowledgements

This research was supported by the Division of Materials Sciences, US Department of Energy under contract DE-AC02-76ER01198. We thank the staff of the Center for Microanalysis of Materials in the Materials Research Laboratory at Urbana for assistance and Dr P. G. Debrunner for the Mössbauer spectroscopy.

References

1. M. W. DAVIES, B. KERRISON, W. E. GROSS, M. J. ROBSON and D. W. WICHALL, *J. Iron Steel Inst.* **208** (1970) 348.
2. C. J. GOODBRAKE, Thesis, Department of Ceramic Engineering, University of Illinois (1975).
3. R. J. LAUF, *Amer. Ceram. Soc. Bull.* **61** (1982) 487.
4. E. M. RABINOVICH, *Adv. Ceram.* **4** (1982) 334.
5. M. A. ALI, "Crystallized Fly Ash Feasibility Study", Electric Power Research Institute, Palo Alto, California, USA, Final Report EL-1836 (1981).
6. G. B. CARRIER, *J. Amer. Ceram. Soc.* **47** (1964) 365.
7. E. E. UNDERWOOD, "Quantitative Stereology" (Addison-Wesley, Reading, Mass., 1970).
8. M. A. KNIGHT, *J. Amer. Ceram. Soc.* **28** (1945) 297.
9. M. E. FINE, "Dynamic Methods for Determining the Elastic Constants and Their Temperature Variation in Metals", ASTM Special Technical Publication 129, (1952) pp. 43–67.
10. P. S. ROGERS and J. WILLIAMSON, *Glass Technol.* **10** (1969) 128.
11. G. H. BEALL and H. L. RITTLER, *Amer. Ceram. Soc. Bull.* **55** (1976) 579.
12. Y. D. KRUCHININ and Y. L. BELOUSOV, *Fiz. Khim. Stekla* **2** (1976) 238.
13. Y. D. KRUCHININ, D. F. KHADYERA and A. V. LUNDINA, *ibid.* **4** (1978) 147.
14. E. M. LEVIN, C. R. ROBBINS and H. F. McMURDIE, "Phase Diagrams for Ceramists", edited by M. K. Reser (American Ceramic Society, Columbus, Ohio, 1969).
15. D. G. HOLLOWAY, "The Physical Properties of Glass" (Wykeham, London, 1973).
16. E. P. POPOV, "Mechanics of Materials", 2nd edn. (Prentice Hall, Englewood Cliffs, New Jersey, 1976).

Received 8 August
and accepted 13 September 1983